nature energy

ARTICLES

PUBLISHED: 17 FEBRUARY 2017 | VOLUME: 2 | ARTICLE NUMBER: 17007

A half-wave rectified alternating current electrochemical method for uranium extraction from seawater

Chong Liu[1], Po-Chun Hsu[1], Jin Xie[1], Jie Zhao[1], Tong Wu[1], Haotian Wang[2†], Wei Liu[1], Jinsong Zhang[1], Steven Chu[3,4] and Yi Cui[1,5*]

In total there is hundreds of times more uranium in sea water than on land, but extracting it for use in nuclear power generation is challenging due to its low concentration (∼3 ppb) and the high salinity background. Current approaches based on sorbent materials are limited due to their surface-based physicochemical adsorption nature. Here we use a half-wave rectified alternating current electrochemical (HW-ACE) method for uranium extraction from sea water based on an amidoxime-functionalized carbon electrode. The amidoxime functionalization enables surface specific binding to uranyl ions, while the electric field can migrate the ions to the electrode and induce electrodeposition of uranium compounds, forming charge-neutral species. Extraction is not limited by the electrode surface area, and the alternating manner of the applied voltage prevents unwanted cations from blocking the active sites and avoids water splitting. The HW-ACE method achieved a ninefold higher uranium extraction capacity (1,932 mg g^{-1}) without saturation and fourfold faster kinetics than conventional physicochemical methods using uranium-spiked sea water.

Nuclear power is a mature technology capable of providing electricity on a large scale without greenhouse gas emissions. It accounted for approximately 20% electricity generation in the US during 2000 to 2013 and 13% worldwide[1,2]. Uranium is the key element for nuclear fuel, so the mining and recovery of uranium is of critical importance. Approximately 7.6 million tons of uranium have been identified on land, whereas there is hundreds of times more uranium in sea water[3–5]. This huge amount of 4.5 billion tons of uranium in sea water could be used to supply nuclear energy for thousands of years[6]. The uranium resource on land is unevenly distributed, so developing technology to extract uranium from sea water would greatly reduce concerns of energy and resource security in countries that do not possess uranium ore resources within their own borders. Moreover, extracting uranium from sea water can potentially reduce the negative environmental impact due to mining processes used to recover land-based uranium resources. Hence there is strong motivation to develop cost- and energy-efficient methods to extract uranium from sea water.

Although the amount of uranium in sea water is massive, the concentration of uranium is only ∼3 ppb (3 μg l^{-1})[5]. To extract uranium from its high salinity background (sea water) is extremely challenging. The general evaluation criteria for sea water uranium extraction methods are capacity, kinetics and selectivity. The current state-of-the-art sorbent materials are amidoxime-based polymers. The amidoxime polymer sorbents with the highest capacities reported showed ∼200 mg g^{-1} capacity in simulated sea water and 3.9 mg g^{-1} capacity in marine tests over a period of 56 days[7–9]. To increase the capacity of sorbents, research has focused on exploring materials with higher surface areas and better surface properties, including inorganic oxides/sulfides[10–14], protein/biomass-based sorbents[15,16], metal–organic frameworks[17,18] and carbon-based sorbents[19–24]. However, there are three intrinsic limitations of the physicochemical adsorption methods. First, due to the low uranium concentration in sea water, the diffusion of uranyl ions to the surface of the sorbents is slow. Second, the adsorbed cations are positively charged and thus would reject the incoming uranyl ions due to Coulomb repulsion, leaving a great portion of the surface active sites inaccessible (Fig. 1a). Last, other cations, such as sodium and calcium, have concentrations many orders of magnitude higher than uranium, which results in strong competition for adsorption active sites. When undesirable species are adsorbed onto the sorbent surface, the active sites would be blocked and reduce the capacity for uranium collection (Fig. 1b).

Here we report the use of the half-wave rectified alternating current electrochemical (HW-ACE) method to extract uranium from sea water. The HW-ACE method solves the conventional drawbacks of physicochemical adsorption by using an electric field to guide the migration of uranyl ions and increase the collision rate onto the sorbents, using electrodeposition to neutralize the charged uranyl ions to avoid Coulomb repulsion, and using an alternating current to avoid the adsorption of unwanted species as well as water splitting. We have achieved a uranium extraction capacity of 1932 mg g^{-1} using spiked real sea water without observing capacity saturation. The HW-ACE method also showed fourfold faster kinetics than physicochemical adsorption. Finally, we have successfully demonstrated uranium extraction in unspiked real sea

[1]Department of Materials Science and Engineering, Stanford University, Stanford, California 94305, USA. [2]Department of Applied Physics, Stanford University, Stanford, California 94305, USA. [3]Department of Physics, Stanford University, Stanford, California 94305, USA. [4]Department of Molecular and Cellular Physiology, Stanford University, Stanford, California 94305, USA. [5]Stanford Institute for Materials and Energy Sciences, SLAC National Accelerator Laboratory, 2575 Sand Hill Road, Menlo Park, California 94025, USA. †Present address: Rowland Institute at Harvard, Harvard University, Cambridge, Massachusetts 02142, USA. *e-mail: yicui@stanford.edu

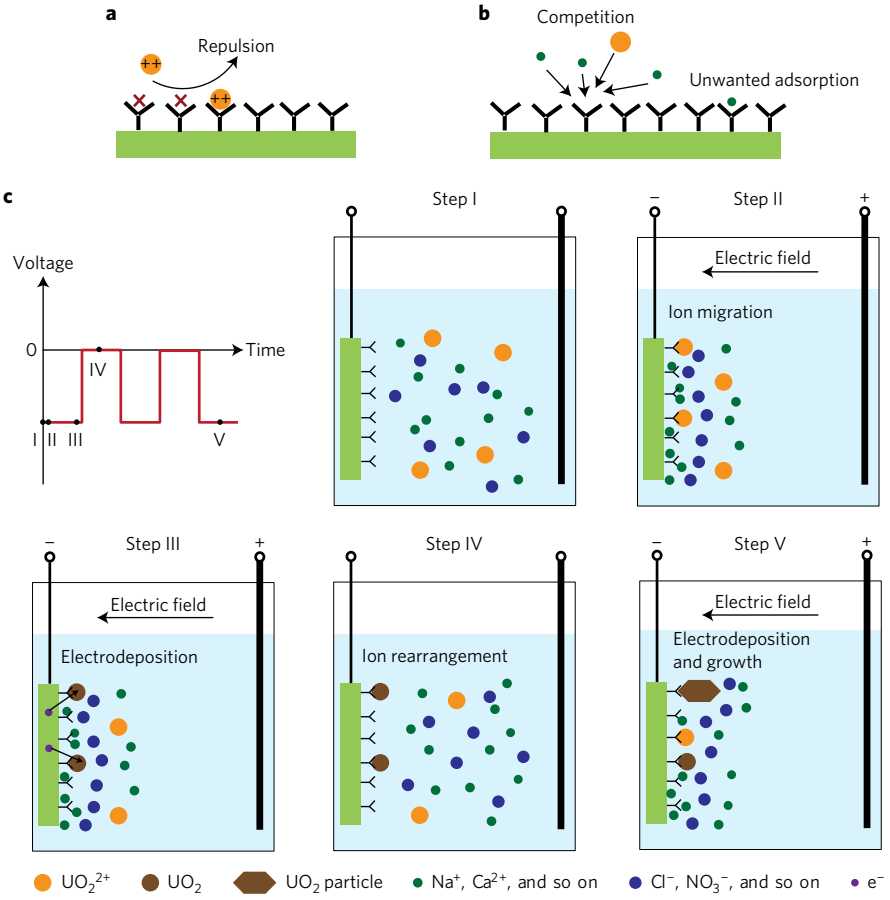

Figure 1 | Schematics of physicochemical and HW-ACE extraction. a, In physicochemical adsorption systems, Coulomb repulsion can cause incoming ions to be rejected by the adsorbed charged ions. **b**, Competition between uranyl ions and other cations reduces the adsorption of uranyl ions and results in blocking of active sites. **c**, Physical processes in HW-ACE extraction. In step I, all ions are dispersed in sea water solution in a random manner. In step II, ions start to migrate according to the external electric field and form an electrical double layer (EDL). Adsorbed uranyl ions can specifically bind to the electrode surface. In step III, adsorbed uranyl ions can be reduced to charge-neutral species such as UO_2. In step IV, when the bias is removed, other ions without specific binding will be rejected to the solution again. In step V, the adsorption and electrodeposition of uranyl ions continues and causes growth of bigger UO_2 particles.

water. The uranium mass extracted by the HW-ACE method was nearly three times that of physicochemical adsorption.

HW-ACE extraction method

The details of the HW-ACE method to extract uranium from sea water are shown in Fig. 1c. An amidoxime-functionalized electrode was used because amidoxime can provide chelation sites that preferably bind to uranyl ions (UO_2^{2+})[25,26]. In HW-ACE extraction an alternating voltage is applied to a C-Ami electrode. The voltage alternates between a negative value and zero with equal duration. The amplitude and frequency can tuned to maximize the extraction performance. The HW-ACE uranium extraction process is explained in five steps in the schematics. In step I, all the ions are randomly distributed in the aqueous solution. In step II, when the negative bias is applied, cations and anions start to migrate under the influence of the external electric field and form an electrical double layer (EDL) on the surface of the amidoxime electrode. (The physical process in the counter electrode is not included for simplicity). The uranyl ions in the inner layer of the EDL can form chelation binding to the electrode surface. In step III, uranium species can be further reduced and electrodeposited as charge-neutral species, such as UO_2. When the bias is removed, in step IV, only the uranyl ions and the electrodeposited UO_2 are left attached to the electrode surface. Other ions without specific binding are redistributed on the electrode surface and release the surface active sites. As the cycle repeats (step V), further uranyl ions attach to the electrode surface and the deposited UO_2 can grow into bigger particles.

To demonstrate this idea, the amidoxime electrode was first fabricated by coating a conductive carbon felt substrate with a blend slurry of polyacrylonitrile (PAN) and activated carbon. The carbon felt substrate is highly conductive, with a fibre diameter of ~20 μm and a pore size ranging from tens to hundreds of micrometres. The function of the nano-size activated carbon (30–50 nm in diameter) is to increase the electrode surface area and, more importantly, to enhance the electrical contact of the amidoxime polymer. PAN was used as a precursor for amidoxime synthesis. A hydrothermal reaction was followed to substitute the nitrile functional groups with amidoxime functional groups (Supplementary Fig. 1)[27]. The scanning electron microscope (SEM) image in Fig. 2a shows the morphology of the C-Ami electrode. The enlarged SEM image in Fig. 2b shows that the carbon felt fibres were covered with a slurry coating of activated carbon and amidoxime. The inset of Fig. 2b shows that the coating itself is also porous, with pore sizes ranging from tens to hundreds of nanometres. These hierarchical pores allow efficient uranyl ion transport and maximize the usage of amidoxime active sites. The existence of amidoxime was confirmed by Fourier transform infrared spectroscopy (FTIR), and the results are shown in Fig. 2c. In the spectrum, peaks at 3,100–3,300 cm^{-1}, 1,635 cm^{-1}, 1,572 cm^{-1} and 912 cm^{-1} represent O–H, C=N, N–H and N–O groups in amidoxime, respectively[27].

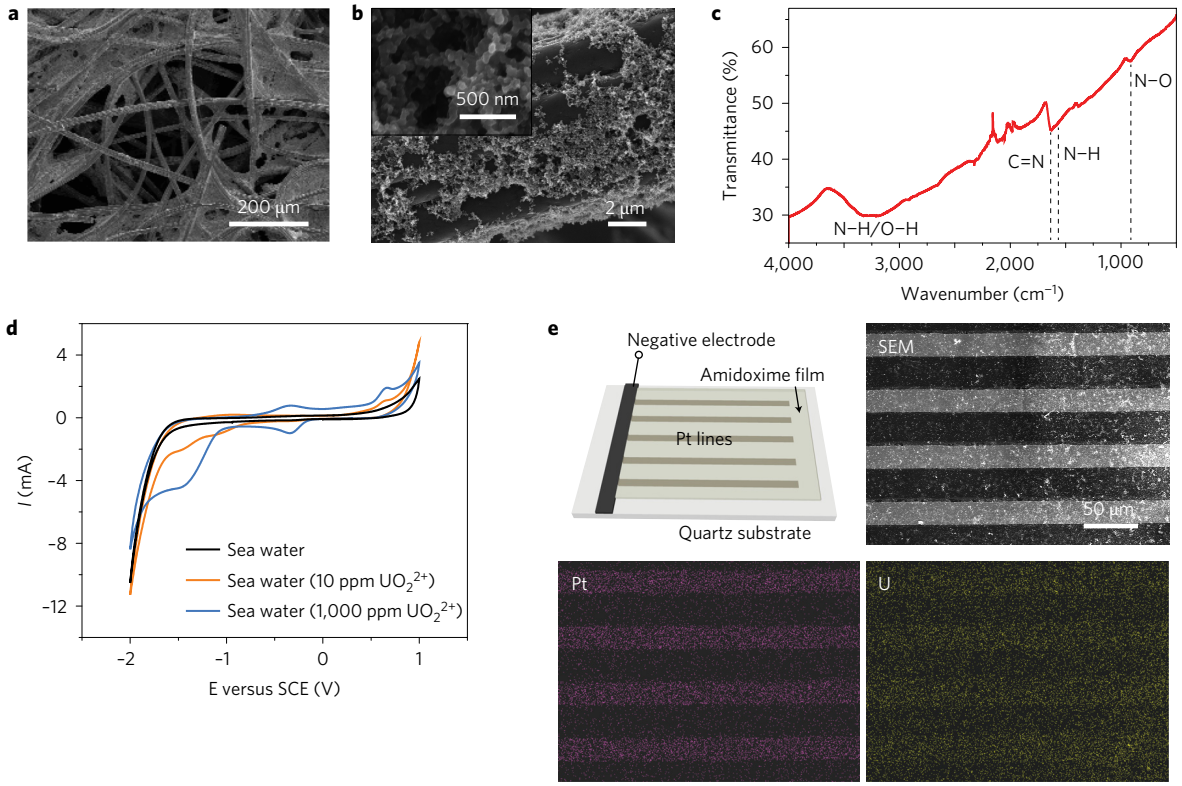

Figure 2 | C-Ami electrode characterization and visualization of the extraction difference between the physicochemical and HW-ACE methods. a, SEM image showing the morphology of the C-Ami electrode. **b**, SEM image showing the surface of the C-Ami electrode with activated carbon and amidoxime polymer. Inset shows the porous structure of the surface coating at a higher magnification. **c**, FTIR spectra of the C-Ami electrode. **d**, Cyclic voltammograms of uranyl-nitrate-spiked real sea water with concentrations of 10 ppm and 1,000 ppm compared to pristine, unspiked real sea water. **e**, The schematic shows the patterned electrode comprising parallel Pt lines on an insulating quartz substrate with a thin layer of amidoxime polymer on top. The corresponding SEM image is also shown. Pt and U EDX element analysis maps on the patterned Pt electrode coated with amidoxime thin film show that the uranium distribution matches the Pt pattern, indicating better extraction efficiency of the HW-ACE method than the traditional physicochemical method. The scale is the same for all images.

The electrochemical characteristics of uranium was studied using cyclic voltammetry (CV), to investigate the uranyl species present during the electrodeposition process. The CV scan curves of real sea water spiked with 10 ppm and 1,000 ppm uranyl nitrate are shown in Fig. 2d, in comparison with unspiked real sea water. All sea water used was filtered through a 0.2-µm filter to remove any microorganisms. In the case of filtered sea water, there was no obvious reduction/oxidation peak, so the peaks appearing in the scan curves of 10 ppm and 1,000 ppm uranyl nitrate can be identified solely as uranium reduction/oxidation reactions. Both 10 ppm and 1,000 ppm uranyl solutions showed a peak at −1.41 V (versus SCE), which represents the reduction of U (VI) to U (V)[28–32]. As for the oxidation reaction, a peak at −0.36 V (versus SCE) for U (V) to U (VI) was observed. The U (V), appearing as UO_2^+ after reduction, can further disproportionate into U (VI) and U (IV) automatically[28]. This is consistent with the fact that the reduction peak of U (VI) to U (V) has a much greater magnitude than the reverse oxidation peak of U (V) to U (VI) because some of the U (V) became U (IV) after formation. Among these three forms of uranium, only U (IV) is insoluble in water and would precipitate out as immobilized UO_2 onto the electrode surface. The electrochemical characterization data confirmed that, with a reducing current, all the U (VI) ions would finally be extracted out as U (IV) in neutral oxide species.

The advantages of the HW-ACE method in comparison to physicochemical adsorption were directly visualized. A patterned electrode of parallel Pt lines was fabricated by photolithography on an insulating quartz substrate, as shown in Fig. 2e. A thin layer of amidoxime polymer was coated on top of the patterned electrode. The amidoxime in contact with the bottom Pt lines would be in HW-ACE extraction, while the remaining lines represent physicochemical adsorption. The HW-ACE extraction parameters were investigated using a C-Ami electrode under different bias voltages and HW-AC frequencies (Supplementary Fig. 2–4). Finally, a square wave with voltages of −5–0 V and a frequency of 400 Hz was chosen based on its fast kinetics and minimum water splitting. After 12 h of extraction, the electrode was characterized by energy-dispersive X-ray spectroscopy (EDX) mapping. The Pt and U element mapping showed that the uranium distribution on the electrode followed the pattern of the Pt, which indicates that the HW-ACE method can extract more uranium than physicochemical adsorption.

Extraction performance in uranium-spiked sea water

To quantitatively evaluate the uranium extraction performance, a series of extraction experiments were conducted, the data of which are shown in Fig. 3a–f and Supplementary Fig. 5. The results reflect the difference in capacity and kinetics between extraction with and without a bias. For the results using real sea water (Half Moon Bay, California, USA) as background solution, the initial concentrations of uranyl ions were ∼150 ppb, ∼1.5 ppm, ∼15 ppm, ∼400 ppm, ∼1,000 ppm and ∼2,000 ppm in the six cases. C-Ami was used as the working electrode and graphite rod as the counter electrode. In all cases, the HW-AC voltage used was −5 V to 0 V with a frequency of 400 Hz. The amount of uranium extracted on C-Ami was evaluated over 24 h. In all

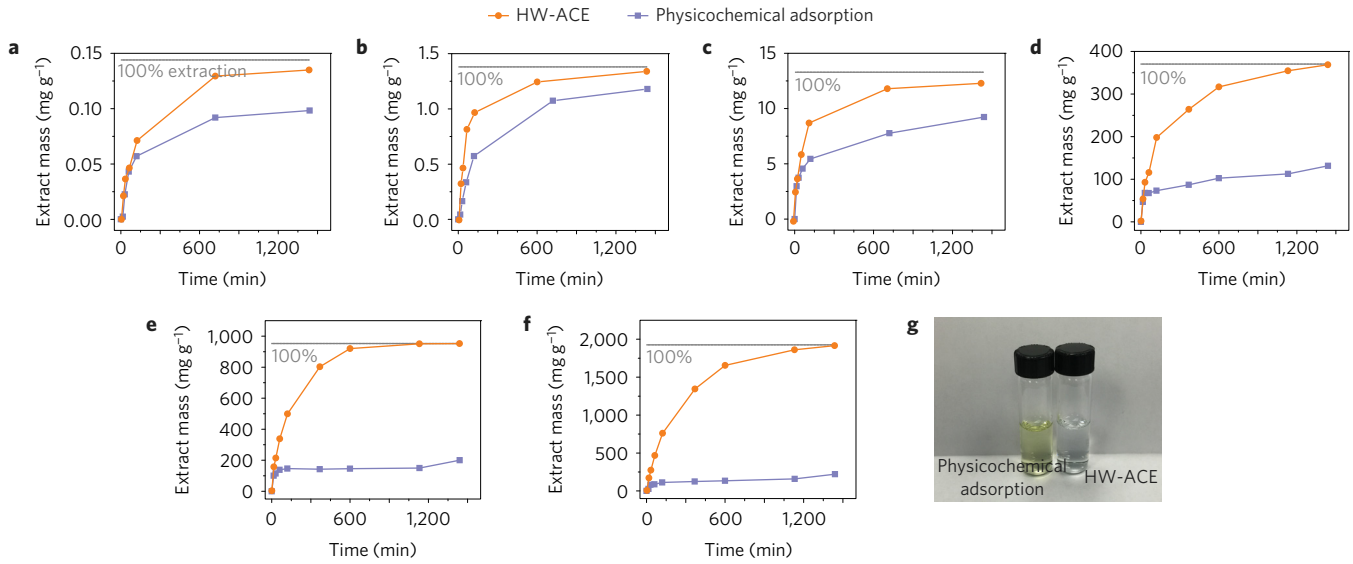

Figure 3 | HW-ACE uranium extraction performance using spiked real sea water. a–f, Uranium extraction from spiked real sea water using the HW-ACE method compared to the physicochemical method with initial uranium concentrations of ~150 ppb (**a**), ~1.5 ppm (**b**), ~15 ppm (**c**), ~400 ppm (**d**), ~1,000 ppm (**e**) and ~2,000 ppm (**f**). **g**, Photo of spiked sea water solutions (initial uranium concentration of ~1,000 ppm) after 24 h of extraction using the HW-ACE and physicochemical methods.

six cases, the mass of uranium extracted by HW-ACE extraction was greater than that from physicochemical adsorption, and the difference became larger with a higher initial concentration. Moreover, for an initial concentration of ~1,000 ppm and above, physicochemical adsorption showed saturation at a capacity of 200–220 mg g^{-1} (g kg^{-1}). In sharp contrast, HW-ACE extraction showed no saturation even at the highest initial concentration tested, which gave an extraction capacity of 1,932 mg g^{-1} (g kg^{-1}) and an extraction efficiency of 99.4%. This high extraction capacity by the HW-ACE extraction was approximately nine times higher than that of physicochemical adsorption. This large capacity difference can be directly identified from the appearance of the uranium sea water solution after extraction. Fig. 3g shows an image of uranium sea water solutions after 24 h of extraction in both HW-ACE and physicochemical extraction, starting with an initial uranyl concentration of ~1,000 ppm. Initially, the solutions appeared to be yellow colour. After extraction, the sea water solution using HW-ACE extraction turned completely clear without any trace of yellow colour. However, in the case of physicochemical adsorption, the yellow colour remained. The C-Ami electrode used in HW-ACE extraction showed no observable damage after use (Supplementary Fig. 6). The extraordinary difference in extraction performance also showed up in the low initial concentration case. Uranium sea water solution with a concentration of 1 ppm was refreshed using either physicochemical or HW-ACE extraction every 24 h (Supplementary Fig. 7). Physicochemical adsorption started to show a decay in extraction efficiency after the second feed, and at the tenth feed the extraction efficiency dropped to 47.3%. In contrast, HW-ACE extraction maintained a high extraction efficiency—on average 99.0% throughout the entire ten cycles. All these results confirm that the HW-ACE method achieved better extraction capacity. If this were carried out with high coulombic efficiency, it could be cost-competitive for real applications (Supplementary Discussion). Besides a much higher capacity, HW-ACE extraction also gave a faster kinetics. The extraction kinetics was analysed for both HW-ACE extraction and physicochemical adsorption with an initial concentration of 1 ppm. Both first-order and second-order reactions were fitted to the experimental data based on the concentration of uranyl ions in the sea water solution, as shown in Supplementary Fig. 8. The experimental data for HW-ACE extraction and physicochemical adsorption both showed better fitting to second-order reaction kinetics. The reaction rate in HW-ACE extraction is approximately four times faster than that of physicochemical adsorption according to a second-order reaction fitting. The quantitative analysis on uranium extraction proved that HW-ACE extraction not only achieved a much higher capacity but also faster kinetics.

Extracted uranium species identification

The extracted uranium species were further characterized to study the HW-ACE extraction mechanism. First, the morphologies of the extracted uranium after 24 h of extraction under both HW-ACE and physicochemical extraction using an initial concentration of 1,000 ppm were characterized by SEM (images are shown in Fig. 4a–d). In the HW-ACE extraction case, the C-Ami electrode was fully covered with micrometre-sized particles (Fig. 4a,b). The micrometre-sized particles appear to be identical, with layered structures and square shapes. However, the appearance of the C-Ami without bias in the physicochemical adsorption did not show much change from the C-Ami before adsorption (Figs 4c,d and 2b). The surface of the C-Ami was smooth without any precipitate formation. This agrees with hypothesis that, in the case of HW-ACE extraction, uranyl ions will be electrodeposited onto the C-Ami electrode, forming charge-neutral oxide species. Through XRD characterization (Fig. 4e), the micrometre-sized particles on the C-Ami electrode surface were identified as $(UO_2)O_2 \cdot 2H_2O$ species (JCPDS 01-081-9033). This is also known as metastudtite, one of the two existing uranium peroxide species[33,34]. However, in the previous electrochemical characterization, the uranyl ions were proposed to be electrodeposited onto the negative electrode to form UO_2. The inconsistency of the electrodeposited species led to further exploration on the HW-ACE deposition process. The first recorded discovery of uranium peroxides was on the surface of UO_2 from nuclear waste, where the formation of $(UO_2)O_2 \cdot xH_2O$ was due to the reaction of UO_2 with H_2O_2[35,36]. During the HW-ACE extraction, there could be H_2O_2 generation from the reduction of the dissolved oxygen on the negative electrode. To check this hypothesis, HW-ACE extraction of uranium in air and in N_2 was compared and Raman spectroscopy was used to identify the uranium species. Uranyl ions in sea water solution, $UO_2(NO_3)_2$ salt, and

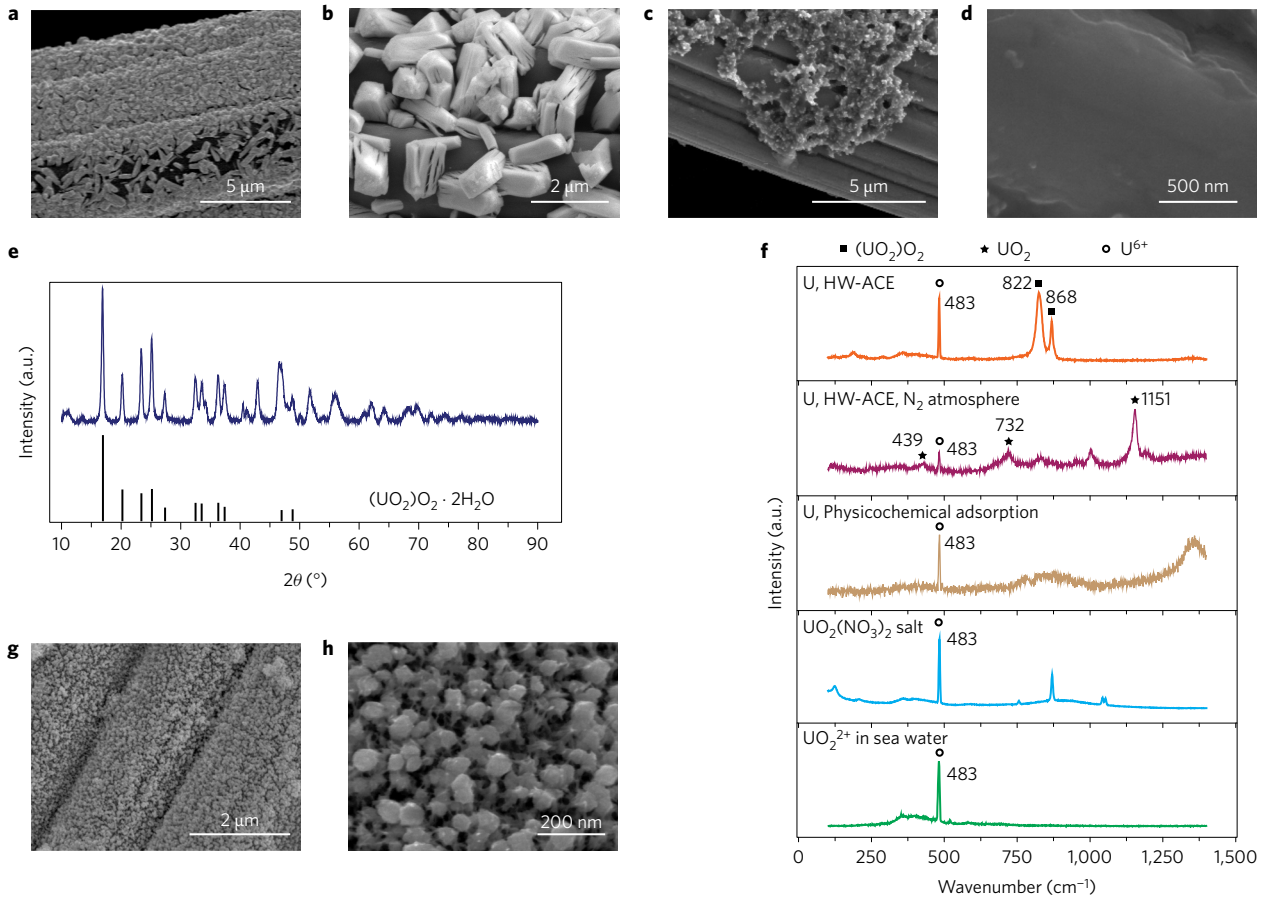

Figure 4 | HW-ACE extraction mechanism study and extracted uranium species analysis. a,**b**, SEM images showing the C-Ami electrode fully covered by particles after 24 h of HW-ACE extraction with an initial uranium concentration of 1,000 ppm. The higher-magnification SEM image (**b**) shows the morphology of the electrodeposited particles. **c**,**d**, SEM images showing the morphology of the C-Ami electrode after 24 h of extraction by the physicochemical method with an initial uranium concentration of 1,000 ppm. **e**, (Top) XRD pattern of the C-Ami electrode after 24 h of HW-ACE extraction. (Bottom) XRD peaks from reference $(UO_2)O_2 \cdot 2H_2O$ (JCPDS 01-081-9033) **f**, Comparison of Raman spectra of the C-Ami electrodes after 24 h of HW-ACE extraction in both air and N_2 environments, and after 24 h of extraction by the physicochemical method, against uranyl nitrate salt (solid) and uranyl nitrate sea water solution. **g**,**h**, SEM images showing the morphology of the C-Ami electrode after 24 h of extraction by the HW-ACE method in a N_2 atmosphere with an initial uranium concentration of 1,000 ppm.

physicochemical adsorbed uranium were characterized by Raman spectroscopy as controls. From the results (Fig. 4f), it can be seen that all the control samples showed a characteristic peak from U^{6+} at ~483 cm^{-1} (refs 37,38). For the HW-ACE extraction in air, two peaks at 822 and 868 cm^{-1} indicate that the uranium species were uranium peroxide, $(UO_2)O_2 \cdot xH_2O$[38]. This is consistent with the XRD result. When HW-ACE extraction was performed in a N_2 atmosphere without O_2, Raman spectroscopy showed different peaks at 439, 732 and 1,151 cm^{-1}, which belong to UO_2[37,38]. This is consistent with the prediction from the electrochemical characterization. The Raman results revealed that, during HW-ACE extraction, uranyl ions adsorbed onto C-Ami were first electrochemically reduced to UO_2, which then reacted with the H_2O_2 generated from the oxygen reduction reaction, so the final extracted uranium species became $(UO_2)O_2 \cdot xH_2O$. Indeed, the UO_2 species from HW-ACE extraction under a N_2 atmosphere showed a different morphology than $(UO_2)O_2 \cdot 2H_2O$, as shown in Fig. 4g,h. The particles attached were spherical with diameters of 50–100 nm. These UO_2 particles were found to be in an amorphous phase by XRD characterization. From the analysis of the extracted uranium species, it can be concluded that whether the recovered uranium becomes UO_2 or $(UO_2)O_2 \cdot 2H_2O$ depends on the water oxygen level. In real applications of sea water uranium extraction, this is determined by the depth in the sea. The extracted U species difference was also confirmed by X-ray photoelectron spectroscopy (XPS) characterization (Supplementary Fig. 9). Nevertheless, either UO_2 or $(UO_2)O_2 \cdot 2H_2O$ are charge-neutral oxide species and could facilitate further electrodeposition to ensure a much larger extraction capacity than the physicochemical adsorption method.

Extraction performance in unspiked real sea water

The HW-ACE method was investigated using real sea water without additional uranium to demonstrate its realistic application. The concentration in the real sea water was tested to be ~3.0 ppb after filtration through a 0.2-µm filter to remove particles and microorganisms. Flow systems were used to measure the U uptake by both HW-ACE and physicochemical adsorption methods. Four litres of sea water was flowed and the U concentration in the effluent was monitored as a function of the volume of water. The accumulated mass of U was plotted with respect to the water volume (Fig. 5a). As shown in the result, after flowing 4 l of sea water, the uptake of U was 1.62 µg and 0.56 µg for the HW-ACE and physicochemical adsorption methods, respectively. The U uptake was three times greater in the case of HW-ACE extraction compared to physicochemical adsorption. To accumulate more U for characterization afterwards, an additional 12 l of real sea water was flowed through each system. The morphology of the C-Ami electrodes in both HW-ACE and physicochemical

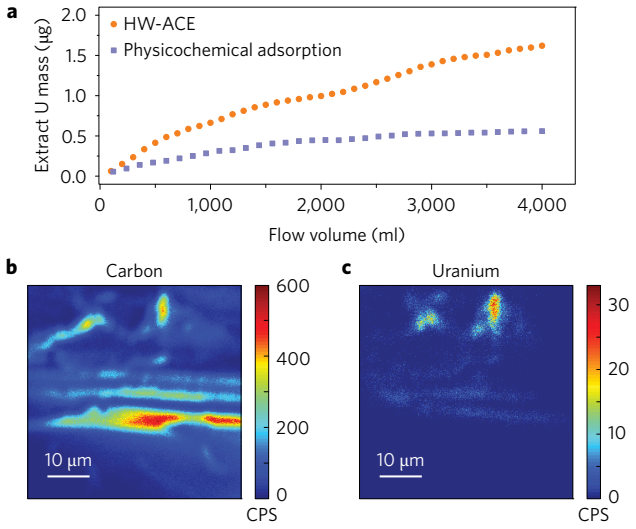

Figure 5 | Unspiked real sea water U extraction. a, Comparison of the long-term U extraction performance between the HW-ACE and physicochemical adsorption methods using flow systems. **b**,**c**, NanoSIMS mapping of C and U, respectively, on the C-Ami electrode after long-term flow experiment in the case of HW-ACE extraction. CPS, counts per second.

adsorption was characterized by SEM, as shown in Supplementary Fig. 10. In the HW-ACE case, the morphology of the electrode did not change much and a few nanoparticles can be observed on the surface of the electrode. To confirm the extraction of U and to obtain the elemental distribution, nanoscale secondary ion mass spectrometry (nanoSIMS) was used to map the electrode surface. For the HW-ACE extraction case, the C and U mappings are shown in Fig. 5b,c. The C signal represents the position of the electrode. As can be seen from the mapping, the U distribution followed the pattern of C, which demonstrated its universal existence on the C-Ami electrode surface. Some spots on the electrode showed higher concentrations of U at a resolution of ~200 nm, which could potentially be due to particle formation. In contrast, because much less U was extracted in the case of physicochemical adsorption, no strong U signal was observed. The nanoSIMS results prove the successful extraction of U by the HW-ACE method. In addition, the kinetics was also evaluated based on real sea water extraction results (Supplementary Fig. 11) using a stationary system. The decrease of U concentration was monitored. On the basis of a second-order reaction fitting, the reaction rate in the HW-ACE case was 2.5 times that of the physicochemical adsorption case. These results prove that in real sea water uranium extraction, the HW-ACE method shows both higher extraction capacity and also higher kinetics than physicochemical adsorption.

Performance with competing ions and desorption

Besides capacity and kinetics, HW-ACE extraction showed high performance for U extraction in the presence of competing ions. Using a solution of uranium spiked in real sea water with an initial concentration of ~1 ppm and in the presence of competing ions (V, Cu and Fe) of the same concentration, the U extraction was investigated. The results are shown in Supplementary Figs 12 and 13. The extraction efficiencies of U, Na and Ca are 78.6%, 1.5% and 1.4% for HW-ACE extraction and 58.5%, 1.2% and 0.9% for physicochemical adsorption, as shown in Supplementary Fig. 13. This result proves that the HW-ACE method yields high extraction of U relative to sodium and calcium from the amidoxime functional group. For the competing ions, V and Fe did not show much difference in extraction efficiency using either the HW-ACE or physicochemical methods. Cu ions in the HW-ACE case showed an increase in extraction of 9% compared to the physicochemical adsorption method. The greatest enhancement was observed for uranium, with the fraction of extracted ions increasing from 58.5% to 78.6% on using HW-ACE extraction. At a similar concentration, the extraction preference ratios (compared by extraction percentage) of U to V, Fe and Cu are 0.93, 1.12 and 0.69 in the physicochemical adsorption case and 1.30, 1.47 and 0.84 in the HW-ACE case. These results showed that the selectivities of U relative to other ions are higher in the HW-ACE case than in the physicochemical adsorption case. This enhancement of U selectivity could be due to the alternating nature of the electric field which could remove unwanted species.

Finally, desorption was conducted to evaluate the percentage of uranium recovered. In traditional physicochemical adsorption, uranyl ions adsorbed on the amidoxime polymer surfaces can be eluted by both Na_2CO_3 and HCl solution with a concentration of 0.1 M. As shown in Supplementary Fig. 14 (cases A and B), Na_2CO_3 (A) and HCl (B) solution can recover 75.6% and 76.0% of uranyl ions after a single cycle of elution. Whereas in the case of HW-ACE extraction, the uranium species attached onto amidoxime polymer surfaces are UO_2 or $(UO_2)O_2 \cdot 2H_2O$, they can only be eluted by HCl solution with a concentration of 0.1 M. As shown in Supplementary Fig. 14 (case C), 0.1 M Na_2CO_3 was used as the elution solution and only 21.6% of uranium can be recovered. Even with a reverse bias (case D), the total uranium recovered is 46.9%. The highest recovery of uranium from HW-ACE extraction was using 0.1 M HCl as elution solution (case F) and with an applied reverse bias. The desorption efficiency was 96.2%. If no reverse bias was applied the desorption efficiency was 82.0% (case E). Therefore, with the optimal desorption condition, 96.2% uranium can be recovered. The desorption of other ions was also evaluated. Using 0.1 M HCl with reverse bias, 90.0%, 91.4% and 97.3% of V, Fe and Cu, respectively, can be recovered (Supplementary Fig. 15). The elution process did not damage the C-Ami electrode and the electrode was reused for three cycles with no observation of extraction capacity loss (Supplementary Fig. 16).

Conclusions

In summary, we designed a method using a half-wave rectified alternating current to electrochemically extract uranium from sea water. This HW-ACE method can overcome the limitations of traditional physicochemical adsorption and simultaneously achieve high extraction capacity, fast kinetics, and high selectivity. Compared to physicochemical adsorption, this HW-ACE extraction method using C-Ami electrode showed a ninefold higher extraction capacity of 1,932 mg g^{-1} and a fourfold faster kinetics. After desorption, 96.2% or uranium can be recovered. This technology showed great potential for efficiently and cost-effectively mining U from sea water. Further optimization of the electrode material and operation system could also enhance its scalability.

Methods

C-Ami electrode fabrication. Carbon felt (Alfa Aesar, 99.0%) was cut into 1 cm^2 circular shapes as electrode substrates. Polyacrylonitrile (Sigma-Aldrich, molecular weight ~150,000), activated carbon was suspended into *N*,*N*-dimethylformamide (DMF) solvent at a mass ratio of 1:1:30. The solution was stirred overnight to form a uniform slurry. The carbon felt substrate was then dip-coated with the slurry and air-dried on a hotplate (70 °C). Then the coated electrode was put into a water bath (25 ml) stabilized at 70 °C. 80 mg ml^{-1} hydroxylamine hydrochloride (Sigma-Aldrich, 99%) and 60 mg ml^{-1} sodium carbonate were added into the water bath quickly and the reaction was allowed to proceed for 90 min (ref. 27). After the reaction, the electrode was washed with deionized water and air-dried in a furnace (80 °C) for use.

Material characterization. Cyclic voltammetry of the C-Ami electrode was carried out using a saturated calomel electrode (SCE) as the reference electrode and a graphite rod (Sigma-Aldrich, 99.995%) as the counter electrode. The scan

rate was 1 mV s^{-1}. Scanning electron microscopy (SEM, FEI Nova NanoSEM 450) with beam energies of 5 kV and 15 kV was used for imaging and EDX mapping, respectively. Fourier transform infrared spectroscopy (FTIR, Nicolet iS50) was carried out in the attenuated total reflectance mode. Raman spectroscopy (WITEC Raman spectrometer) was conducted using a 532 nm excitation laser. XRD (PANalytical Material Research Diffractometer) was carried out using Cu Kα radiation. X-ray photoelectron spectroscopy (XPS, SSI SProbe XPS spectrometer) was carried out using an Al (Kα) source. Nanoscale secondary ion mass spectrometry (nanoSIMS, CAMECA) was used for element mapping with a lateral resolution of ~200 nm. For EDX characterization, interdigitated Pt electrodes were prepared by means of a typical lithographic technology. A 1 μm Shipley 3612 Photoresist was first spin-coated on quartz wafers, followed by exposure and development. Hexamethyldisilazane (HMDS) was used as an adhesion promoter to help the resist stick to the wafer surface. Subsequently, a metal layer of Pt with a thickness of 100 nm was deposited on the wafer by means of an e-gun/beam evaporator (Kurt J. Lesker Company). The photoresist was then removed in acetone. The Pt lines are 30 μm in diameter.

Uranium extraction experiment. Spiked uranium solutions were made by dissolving uranyl nitrate salt (VWR, reagent grade) into real sea water collected from Half Moon Bay (California, USA) to different concentrations. The sea water used was filtered through a 0.2-μm filter to remove particles and microorganisms. During HW-ACE extraction, a C-Ami electrode was used as the negative electrode and a graphite rod as the positive electrode. In each adsorption experiment, 15 ml of spiked uranium solution was used. The uranium concentration was measured by inductively coupled plasma mass spectrometry (ICP-MS). The absorbed uranium mass was calculated by comparing the uranium concentration difference before and after adsorption. For HW-ACE extraction in a N_2 atmosphere, the beaker was sealed with spiked uranium solution, with the C-Ami and graphite rod electrodes immersed in it, and with electrical connections left out. Before extraction, N_2 was flowed into the beaker overnight to remove dissolved oxygen. The N_2 purging continued until the extraction finished. For the long-term flow experiment, unspiked real sea water after 0.2-μm filtration was used. A C-Ami electrode (1 cm^2) was used as the negative electrode and C felt (1 cm^2) was used as the positive electrode. These two electrodes were placed in parallel with a tissue paper between as a separator. In the case of HW-ACE extraction, an a.c. voltage of −5 V to 0 V was used with a frequency of 400 Hz. For physicochemical adsorption, no voltage was applied. The filtration rate was maintained at 0.1 cm s^{-1}.

Data availability. The data that support the plots within this paper and other findings of this study are available from the corresponding author upon reasonable request.

Received 13 March 2016; accepted 12 January 2017; published 17 February 2017

References

1. *Annual Energy Outlook 2015 With Projections to 2040* (DOE, 2015); http://www.eia.gov/outlooks/aeo/pdf/0383(2015).pdf
2. Chu, S. & Majumdar, A. Opportunities and challenges for a sustainable energy future. *Nature* **488**, 294–303 (2012).
3. Schenk, H. J., Astheimer, L., Witte, E. G. & Schwochau, K. Development of sorbers for the recovery of uranium from seawater. 1. Assessment of key parameters and screening studies of sorber materials. *Separ. Sci. Technol.* **17**, 1293–1308 (1982).
4. Astheimer, L., Schenk, H. J., Witte, E. G. & Schwochau, K. Development of sorbers for the recovery of uranium from seawater. 2. The accumulation of uranium from seawater by resins containing amidoxime and imidoxime functional groups. *Separ. Sci. Technol.* **18**, 307–339 (1983).
5. Tabushi, I., Kobuke, Y. & Nishiya, T. Extraction of uranium from seawater by polymer-bound macrocyclic hexaketone. *Nature* **280**, 665–666 (1979).
6. Davies, R. V., Kennedy, J., Hill, K. M., McIlroy, R. W. & Spence, R. Extraction of uranium from sea water. *Nature* **203**, 1110–1115 (1964).
7. Kim, J. *et al.* Uptake of Uranium from seawater by amidoxime-based polymeric adsorbent: field experiments, modeling, and updated economic assessment. *Ind. Eng. Chem. Res.* **53**, 6076–6083 (2014).
8. Das, S. *et al.* Extracting uranium from seawater: promising AF series adsorbents. *Ind. Eng. Chem. Res.* **55**, 4110–4117 (2016).
9. Brown, S. *et al.* Uranium adsorbent fibers prepared by atom-transfer radical polymerization (ATRP) from Poly(vinyl chloride)-co-chlorinated Poly(vinyl chloride) (PVC-co-CPVC) fiber. *Ind. Eng. Chem. Res.* **55**, 4139–4148 (2016).
10. Ma, S. L. *et al.* Efficient uranium capture by polysulfide/layered double hydroxide composites. *J. Am. Chem. Soc.* **137**, 3670–3677 (2015).
11. Manos, M. J. & Kanatzidis, M. G. Layered metal sulfides capture uranium from seawater. *J. Am. Chem. Soc.* **134**, 16441–16446 (2012).
12. Gunathilake, C., Gorka, J., Dai, S. & Jaroniec, M. Amidoxime-modified mesoporous silica for uranium adsorption under seawater conditions. *J. Mater. Chem. A* **3**, 11650–11659 (2015).
13. Yang, D. J., Zheng, Z. F., Zhu, H. Y., Liu, H. W. & Gao, X. P. Titanate nanofibers as intelligent absorbents for the removal of radioactive ions from water. *Adv. Mater.* **20**, 2777–2781 (2008).
14. Comarmond, M. J. *et al.* Uranium sorption on various forms of titanium dioxide—influence of surface area, surface charge, and impurities. *Environ. Sci. Technol.* **45**, 5536–5542 (2011).
15. Zhou, L. *et al.* A protein engineered to bind uranyl selectively and with femtomolar affinity. *Nat. Chem.* **6**, 236–241 (2014).
16. Barber, P. S., Kelley, S. P., Griggs, C. S., Wallace, S. & Rogers, R. D. Surface modification of ionic liquid-spun chitin fibers for the extraction of uranium from seawater: seeking the strength of chitin and the chemical functionality of chitosan. *Green Chem.* **16**, 1828–1836 (2014).
17. Carboni, M., Abney, C. W., Liu, S. B. & Lin, W. B. Highly porous and stable metal-organic frameworks for uranium extraction. *Chem. Sci.* **4**, 2396–2402 (2013).
18. Bai, Z. Q. *et al.* Introduction of amino groups into acid-resistant MOFs for enhanced U(VI) sorption. *J. Mater. Chem. A* **3**, 525–534 (2015).
19. Zhao, G. X. *et al.* Preconcentration of U(VI) ions on few-layered graphene oxide nanosheets from aqueous solutions. *Dalton Trans.* **41**, 6182–6188 (2012).
20. Shao, D. D. *et al.* PANI/GO as a super adsorbent for the selective adsorption of uranium(VI). *Chem. Eng. J.* **255**, 604–612 (2014).
21. Wang, F. *et al.* A graphene oxide/amidoxime hydrogel for enhanced uranium capture. *Sci. Rep.* **6**, 19367 (2016).
22. Gorka, J., Mayes, R. T., Baggetto, L., Veith, G. M. & Dai, S. Sonochemical functionalization of mesoporous carbon for uranium extraction from seawater. *J. Mater. Chem. A* **1**, 3016–3026 (2013).
23. Yue, Y. F. *et al.* Polymer-coated nanoporous carbons for trace seawater uranium adsorption. *Sci. China Chem.* **56**, 1510–1515 (2013).
24. Yue, Y. F. *et al.* Seawater uranium sorbents: preparation from a mesoporous copolymer initiator by atom-tansfer radical polymerization. *Angew. Chem. Int. Ed.* **52**, 13458–13462 (2013).
25. Vukovic, S., Watson, L. A., Kang, S. O., Custelcean, R. & Hay, B. P. How amidoximate binds the uranyl cation. *Inorg. Chem.* **51**, 3855–3859 (2012).
26. Barber, P. S., Kelley, S. P. & Rogers, R. D. Highly selective extraction of the uranyl ion with hydrophobic amidoxime-functionalized ionic liquids via η^2 coordination. *RSC Adv.* **2**, 8526–8530 (2012).
27. Saeed, K., Haider, S., Oh, T. J. & Park, S. Y. Preparation of amidoxime-modified polyacrylonitrile (PAN-oxime) nanofibers and their applications to metal ions adsorption. *J. Membr. Sci.* **322**, 400–405 (2008).
28. Hennig, C., Ikeda-Ohno, A., Emmerling, F., Kraus, W. & Bernhard, G. Comparative investigation of the solution species $U(CO_3)_5^{6-}$ and the crystal structure of $Na_6\ U(CO_3)_5 \cdot 12H_2O$. *Dalton Trans.* **39**, 3744–3750 (2010).
29. Ikeda, A. *et al.* Comparative study of uranyl(VI) and -(V) carbonato complexes in an aqueous solution. *Inorg. Chem.* **46**, 4212–4219 (2007).
30. Guin, S. K., Ambolikar, A. S. & Kamat, J. V. Electrochemistry of actinides on reduced graphene oxide: craving for the simultaneous voltammetric determination of uranium and plutonium in nuclear fuel. *RSC Adv.* **5**, 59437–59446 (2015).
31. Kim, Y. K., Lee, S., Ryu, J. & Park, H. Solar conversion of seawater uranium (VI) using TiO_2 electrodes. *Appl. Catal. B Environ.* **163**, 584–590 (2015).
32. Gupta, R., Jayachandran, K. & Aggarwal, S. K. Single-walled carbon nanotube (SWCNT) modified gold (Au) electrode for simultaneous determination of plutonium and uranium. *RSC Adv.* **3**, 13491–13496 (2013).
33. Burns, P. C. & Hughes, K. A. Studtite, $[(UO_2)(O_2)(H_2O)_2](H_2O)_2$: the first structure of a peroxide mineral. *Am. Mineral.* **88**, 1165–1168 (2003).
34. Kubatko, K. A. H., Helean, K. B., Navrotsky, A. & Burns, P. C. Stability of peroxide-containing uranyl minerals. *Science* **302**, 1191–1193 (2003).
35. Wilbraham, R. J., Boxall, C., Goddard, D. T., Taylor, R. J. & Woodbury, S. E. The effect of hydrogen peroxide on uranium oxide films on 316L stainless steel. *J. Nucl. Mater.* **464**, 86–96 (2015).
36. Corbel, C. *et al.* Addition versus radiolytic production effects of hydrogen peroxide on aqueous corrosion of UO_2. *J. Nucl. Mater.* **348**, 1–17 (2006).
37. Manara, D. & Renker, B. Raman spectra of stoichiometric and hyperstoichiometric uranium dioxide. *J. Nucl. Mater.* **321**, 233–237 (2003).
38. Pointurier, F. & Marie, O. Use of micro-Raman spectrometry coupled with scanning electron microscopy to determine the chemical form of uranium compounds in micrometer-size particles. *J. Raman Spectrosc.* **44**, 1753–1759 (2013).

Acknowledgements

We acknowledge the DOE Office of Nuclear Energy for funding. We acknowledge the Stanford facilities, SNSF and EMF, for characterization. We acknowledge C. Hitzman for his help in NanoSIMS characterization.

Author contributions

C.L. and Y.C. conceived the concept. C.L. synthesized the C-Ami electrodes, conducted the electrode characterization and measured the performances. P.-C.H. helped with the FTIR and XRD characterization. J.X. helped with the Raman characterization. J.Z. and H.W. helped with the XPS characterization. T.W. helped with performance measurements. W.L. helped with patterned electrode fabrication. S.C. and Y.C supervised the project. C.L., S.C. and Y.C. analysed the data and co-wrote the paper. All authors discussed the whole paper.

Additional information

Supplementary information is available for this paper.

Reprints and permissions information is available at www.nature.com/reprints.

Correspondence and requests for materials should be addressed to Y.C.

How to cite this article: Liu, C. *et al.* A half-wave rectified alternating current electrochemical method for uranium extraction from seawater. *Nat. Energy* **2**, 17007 (2017).

Competing interests

The authors declare no competing financial interests.